ACS Partner Journal

CHEM & BIO ENGINEERING

pubs.acs.org/ChemBioEng

Article

Spiropyran-Incorporated Y Zeolite: A Visible-Light-Responsive System for Controllable CO adsorption

Published as part of Chem & Bio Engineering virtual special issue "Advanced Separation Materials and Processes".

Shu Shi, Zi-Da Ma, Yu-Xia Li, Shi-Chao Qi, and Lin-Bing Sun*

Cite This: *Chem Bio Eng.* 2024, 1, 783−789

Read Online

ACCESS | Metrics & More | Article Recommendations | Supporting Information

ABSTRACT: The development of high-performance adsorbents is vital for adsorptive separation. Conventional adsorbents have limitations in combining selective adsorption and efficient desorption due to their fixed surface properties. In this work, we have constructed spiropyran (SP)-based visible-light-responsive adsorbents for controllable CO adsorption by synthesizing SP in situ in Y zeolite via the ship-in-the-bottle method. This avoids the drawbacks associated with the vast majority of systems that modulate adsorption capacity by UV light. SP molecules can undergo reversible isomerization within the Y zeolite, which exhibit the merocyanine (MC) state in the dark and revert to the SP form upon visible light stimulation. The results show that the isomerization of MC to SP leads to a tunable CO adsorption capacity of up to 34%. Simulations performed by density functional theory reveal that MC is more likely to trap CO molecules than SP due to its higher binding energy with CO. We further demonstrate that the isomerization-induced tunable adsorption capacity can be maintained during cycles without degradation.

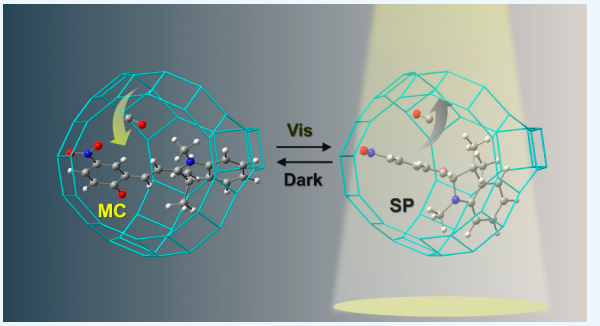

KEYWORDS: *spiropyran, CO adsorption, Y zeolite, visible-light-responsive, selective adsorption*

1. INTRODUCTION

Separation plays an important role in chemical production process.[1,2] As the dominant means of separation, however, distillation in general is energy-intensive, accounting for over half of the total energy consumption of production.[3] The adsorption separation technology is gaining wide attention owing to its low cost, simplicity of operation, and efficient utilization of energy. The exploitation of high-efficiency adsorbents is essential for adsorption separation process.[4−7] An optimal adsorbent should have high selectivity for efficient adsorption of adsorbates and release the adsorbed substance with relative ease. Nevertheless, there is seldom an equilibrium, or even a paradox, between effective adsorption and easy desorption.[8,9] To be more specific, adsorbents with well-defined active sites have strong adsorbent-adsorbate interactions that facilitate adsorption, while making it difficult to desorb the adsorbent, thus leading to significant energy consumption. On the contrary, weak adsorbate−adsorbent interactions favor desorption, but adsorption selectivity is low and product purity requirements are rarely met. Conventional means of modulating adsorption capacity rely on varying pressure or temperature to achieve cyclic changes in adsorption capacity,[10] with considerable energy consumption. There is an urgent need to develop a low-energy method to optimize the trade-off between adsorption and desorption.[11,12]

Motivated with the ability of organisms in the marvelous natural world to adjust accordingly when subjected to external stimuli, scientists have designed stimulus-responsive functional materials capable of changing their structure or properties for use in the fields of sensing, drug delivery, catalysis, and adsorptive separations.[8,13−15] The primary external stimuli include light, heat, pH, pressure, etc., of which light can be considered highly attractive.[16−19] Light is a stimulus delivered immediately to a precise location and comes in the form of different wavelengths, to which different light-responsive molecules respond selectively.[20] However, for the most part, activation of photoresponsive molecules (such as diarylethenes and azobenzenes) requires UV radiation.[21−25] The potentially destructive nature of UV light and its low light penetration depth limit the applicability of materials. Whereas visible light

Received: January 18, 2024
Revised: March 26, 2024
Accepted: April 9, 2024
Published: April 17, 2024

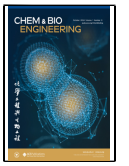

https://doi.org/10.1021/cbe.4c00016
Chem Bio Eng. 2024, 1, 783−789

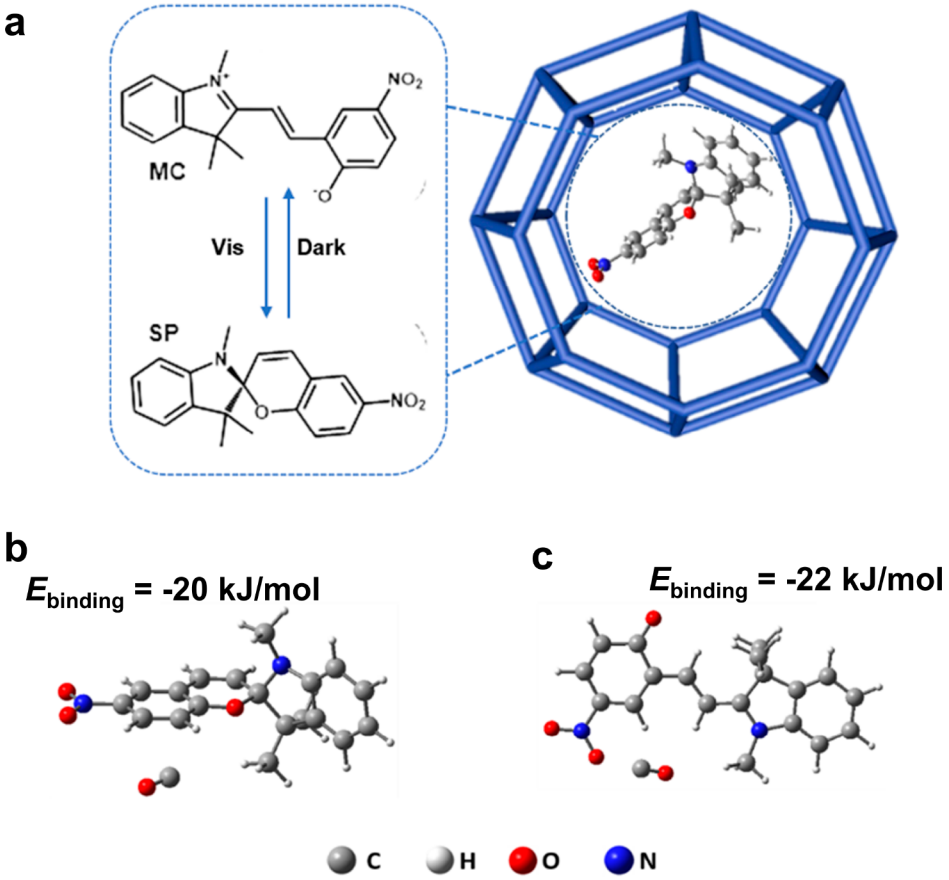

Figure 1. (a) SP-embedded Y zeolite with photo-responsiveness. C, gray; N, blue; O, red; and Cr, cyan. DFT calculations of optimized configurations of CO with (b) SP and (c) MC.

dominates the solar spectrum and circumvents the drawbacks of UV light to some extent, making it more viable for practical applications.[11,26−29] Spiropyrans have attracted more attention due to their unique properties. Upon certain stimuli, the ring-closed spiropyran (SP) form isomerizes to the open merocyanine (MC) form, and the two isomeric forms have very different physicochemical properties. The dihydroindole and chromene portions of the SP form are located perpendicularly on either side of the spiro C−O bond, and these two portions are not conjugated. The MC form is obtained by the SP form undergoing a pericyclic reaction of $2\pi + 2\pi + 2\pi$ that cleaves the spiro C−O bond. During this process, the dipole moment jumps from 4−6 D to 14−18 D with a significant increase in polarity.[30−33] This offers the possibility of modulating the adsorption capacity of porous materials by inducing the SP group, providing a potential energy-saving alternative to pressure and temperature fluctuations.[19,34,35]

Herein, we present for the first time the visible-light-responsive SP-incorporated smart adsorbents for CO adsorption modulation. In situ synthesis of SP in the cage of Y zeolite by the ship-in-bottle method has been employed to prepare SP@Y adsorbents (Figure 1). The Y zeolite has a large intraluminal diameter, thus providing space for the in situ synthesis of SP in the cage as well as its isomerization, along with a small window size, which can confine the SP well within the pore cage.[36,37] The polarity of the reaction cavity provided by the zeolite host facilitates the MC state as the predominant form. Upon visible light, the MC state isomerized into the SP state, followed by removal of visible light placed in the dark the SP state reverted back to the MC state. CO adsorption tests showed a 34% increase in the uptake of CO by the adsorbent upon transformation of the stabilized MC state into the SP state. Density Functional Theory (DFT) calculations revealed that spiropyran molecules with different isomers have distinguished interactions with CO, in agreement with the experimental results. Such smart adsorbents exhibited modulation of CO adsorption capacity with avoidance of the utilization of UV light, which cannot be performed by conventional light-responsive adsorbents.

2. EXPERIMENTAL SECTION

2.1. Materials Preparation. The materials SP@Y was prepared by a ship-in-the-bottle method. As per the previous report,[37] NiY (1 g), 1,3,3-trimethyl-2-methylene indoline (0.5, 1, or 1.5 mmol), and ethanol (20 mL) were stirred in a beaker for 2.5 h. Then 5-nitrosalicylaldehyde (1, 2, or 3 mmol) was added to the fully mixed solution and continue stirring for 2.5 h. The mixture was sonicated for 20 min at room temperature. After washing with ethanol until the supernatant was colorless, the solid was vacuum dried at 80 °C overnight to obtain *n*SP@Y (*n* represents the amount of SP theoretically synthesized on NiY in the unit mmol/g and corresponds to 0.5, 1 and 1.5, respectively).

2.2. Gas Adsorption Tests. A BELSORP-Max analyzer was employed to determine the adsorption isotherms of CO and N_2 Adsorption measurements were performed using CO (99.999%) and N_2 (99.999%) gases each of these samples was tested individually in a water bath for the single-component gas adsorption isotherms in the MC and SP isomerization states at 25 °C. In order to test the adsorption properties of samples with SP states, the sample tubes

https://doi.org/10.1021/cbe.4c00016
Chem Bio Eng. 2024, 1, 783−789

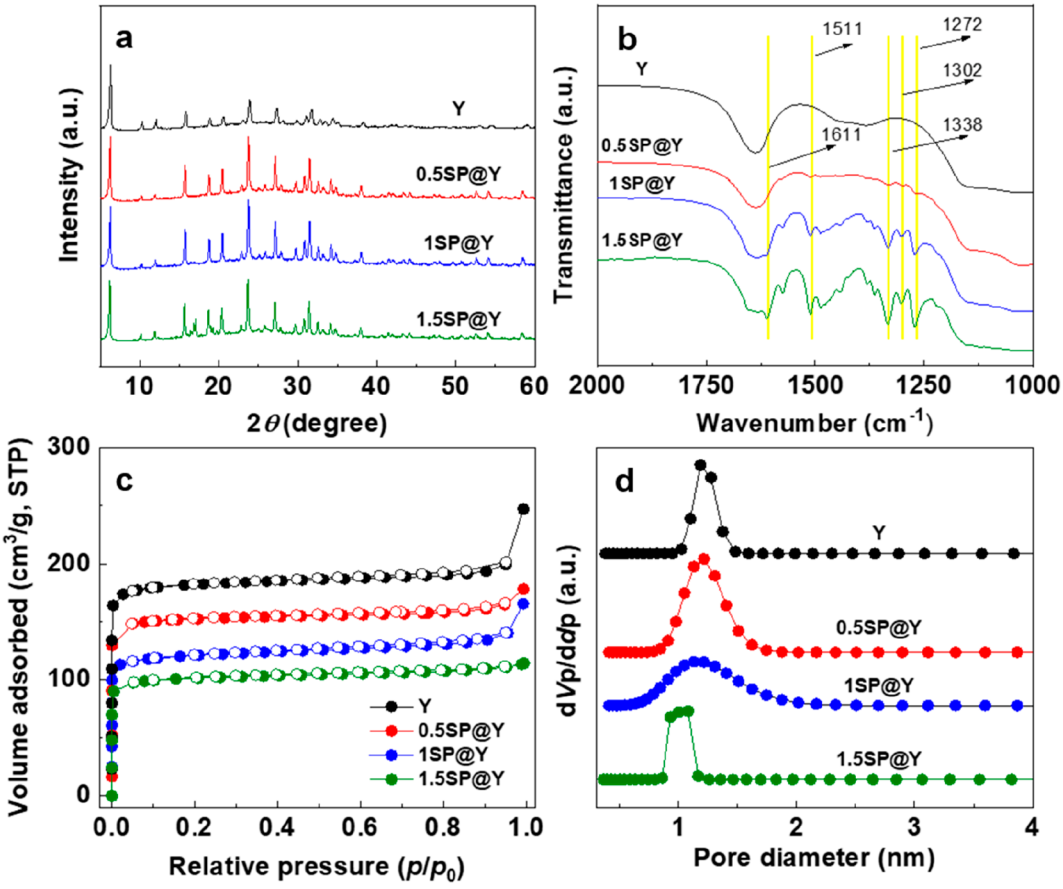

Figure 2. (a) XRD patterns, (b) FTIR spectra, (c) N_2 adsorption−desorption isotherms, and (d) pore size distributions of different samples.

were irradiated with 450 nm visible light during the test. The MC isomeric state test condition refers to the samples were kept in the dark for 3 h after removing the visible light and then carried out to perform adsorption throughout the darkness. The samples were degassed at 120 °C for 10 h prior to analysis. After processing, the samples under MC and SP states were backfilled with N_2 and transferred to the analytical system. The free space was determined using He (99.999%), assuming that He could not be adsorbed at the investigated temperatures.

3. RESULTS AND DISCUSSION

3.1. Structural and Surface Properties. SP@Y was synthesized by introducing SP into the pores of dewatered Y zeolite using the ship-in-the-bottle method. SP can be accommodated within the spherical super-cavity (1.4 nm diameter) of the Y zeolite, however, the dimensions of the SP molecules are too large to pass through the smaller cage window (0.74 nm diameter) directly within the organic solvent and into the carrier. In order to check the effect of the introduction of SP on the Y zeolite, X-ray diffraction (XRD) analysis of SP@Y was carried out (Figure 2a). Compared with Y zeolite, the appearance of all characteristic peaks of SP@Y remains almost unchanged, indicating that the in situ synthesis of SP in the Y zeolite cavity has not disrupted the structure of the carrier. Figure S1 of the Supporting Information shows the SEM and TEM images of samples Y and 1SP@Y. As can be seen, the samples have an ortho-polyhedral shape with a uniform particle size distribution and crystal diameters in the range of 0.2−0.3 μm. Following the loading of SP, the morphology of 1SP@Y does no change, demonstrating that the morphology is well maintained after the introduction of SP into the pores of Y. The dark-field TEM and EDX patterns of 1SP@Y clearly confirm that the N elements are homogeneously distributed within the skeleton of Y.

Figure 2b shows the Fourier transform infrared spectra (FTIR) of different samples. For SP@Y, in addition to the characteristic peaks of Y zeolite, some new characteristic peaks can be detected. The bands at 1272 and 1302 cm^{-1} are the stretching vibration peak and bending vibration peak of C−O and C−N in the SP hexaheterocycle, respectively. Asymmetric vibrational absorption peak of CH_3−C−CH_3 gem-dimethyl on the five-membered heterocyclic ring of the SP molecule is assigned to the absorption peak at 1338 cm^{-1}. This peak at 1511 cm^{-1} is ascribed to the stretching vibration peak of the carbon−carbon unsaturated double bond C═C in the molecule. It is shown that the peak at 1611 cm^{-1} is attributable to the stretching vibrational peaks and bending vibrational peaks of C═C and C═N.[38] Each of these peaks is gradually enhanced with the increase of the introduced SP content, which indicates the successful incorporation of SP molecules into the Y. The pore structure of the sample was determined by N_2 adsorption, Figure 2c provides the N_2 adsorption of the support Y and SP@Y at −196 °C. All samples exhibit N_2 adsorption−desorption isotherms of typical type I. The N_2 adsorption rises rapidly in the low-pressure region, demonstrating that the samples are microporous materials. The N_2 adsorption capacity of the support Y is 247.3 cm^3/g. As the increasing concentration of SP, the adsorption capacity of sample for N_2 decreases. When increasing SP from 0.5 mmol/g to 1.5 mmol/g, the N_2 adsorption capacity of the material decreased from 177.6 cm^3/g to 113.9 cm^3/g, probably because

https://doi.org/10.1021/cbe.4c00016
Chem Bio Eng. 2024, 1, 783−789

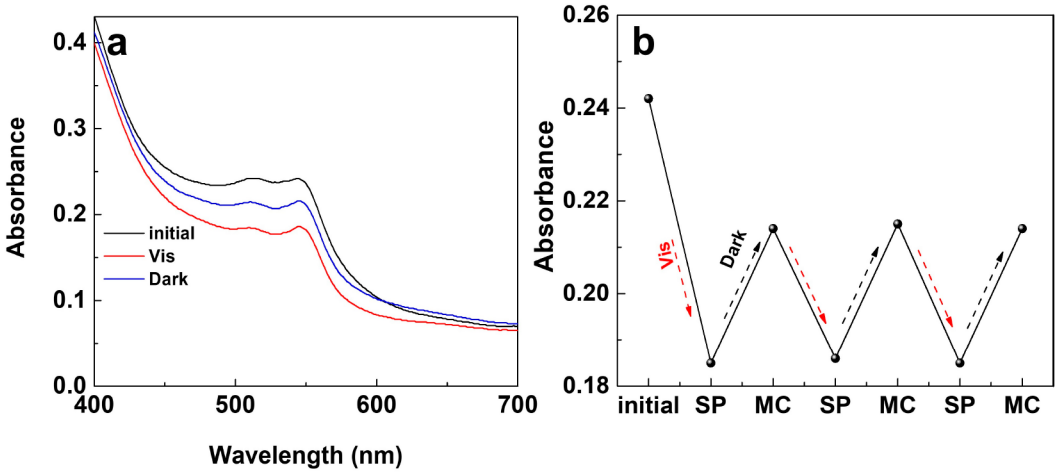

Figure 3. (a) Changes in UV-Vis spectra of 1SP@Y upon MC and SP isomerization. (b) Reversible changes in absorbance at 545 nm as a function of cycles for 1SP@Y.

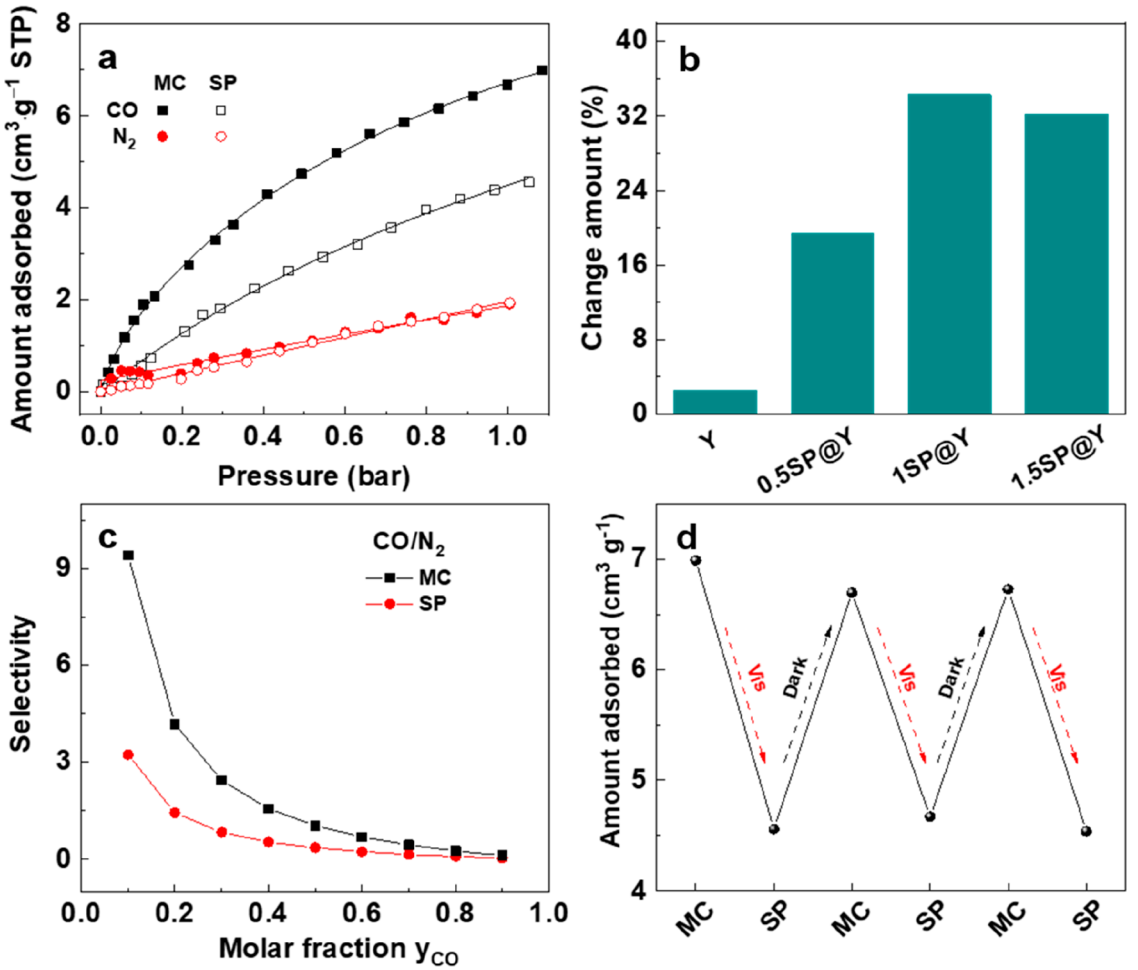

Figure 4. (a) Adsorption isotherms of CO and N_2 on 1SP@Y at 25 °C upon SP/MC isomerization. The lines are fitted using the dual Langmuir model. (b) Changes of CO adsorption capacity on Y and SP@Y at 25 °C upon SP/MC isomerization. (c) IAST selectivity of CO/N_2 on 1SP@Y at 25 °C. (d) Adsorption cycles of 1SP@Y for CO at 25 °C upon SP/MC isomerization.

the introduced SP molecules occupied part of the pores of the Y. From the pore size distribution (Figure 2d), the SP@Y pore size decreased as the amount of SP introduction increased. This further demonstrates the successful in situ synthesis of SP inside the Y cage.

Thermogravimetric analysis (TGA) data can be used to characterize the change in the thermal stability of the carrier following the introduction of SP, as shown in Figure S2. For the carrier Y, when the temperature is 25−200 °C, there is obvious weight loss, and the source of weight loss in this part is mainly the removal of adsorbed water in the material pores.

https://doi.org/10.1021/cbe.4c00016
Chem Bio Eng. 2024, 1, 783−789

Because the carrier has good thermal stability, there is almost no weight loss between 200 and 800 °C. Whereas for SP@Y, the weight loss of the material gradually rises after 200 °C along with the amount of SP added. This is attributed to the fact that SP continuously decomposes and is taken away by air oxidation after 200 °C. TGA was used to further calculate the SP content and the results are listed in Table S1. Quality fractions of SP in 0.5SP@Y, 1SP@Y, and 1.5SP@Y are 5.88, 7.63, and 9.59 wt %, respectively.

On the basis of the above analysis, we have successfully introduced the SP into the pores of the Y, and successfully maintained the original structure of the Y.

3.2. Photo-Responsive Behavior. The photo-response properties of 1SP@Y were evaluated using a UV-Vis spectrophotometer. As shown in Figure 3, an adsorption band was observed at 500 nm to 600 nm, the appearance of this adsorption band is due to the planar structure and extended π-conjugation between the methylene benzhydryl and indoline moieties of the merocyanine leading to the band gap is reduced. It can be seen that the illumination decreased the intensity of the adsorption band, while the dark condition enhanced the intensity of the adsorption band. Moreover, the characteristic peaks have not completely disappeared, indicating that the conversion from MC to SP is incomplete. This could be attributed to the polar environment of the zeolite cavities.[36] As the storage time of the sample in the dark (at 25 °C) increases, the SP gradually transitions to the MC state, reaching stability after 3 h (Figure S3). However, the characteristic peaks did not completely return to the original state after 3 h of storage under dark conditions, which may be that the energy provided by the darkness to transform the MC was not enough to completely restore it to the initial high energy state. Multiple alterations of 1SP@Y by visible light irradiation or storage in darkness revealed that although it could not be fully restored to the original state, the transition between the SP and partial MC states could be kept stable during the remaining 3 cycles excluding the initial state. This can prove that the sample is photoresponsive and can achieve a reversible cycle of SP isomerization by switching the conditions. To expedite the isomerization process in the dark, the isomerization time of the sample at 45 °C was investigated. It was found that at this temperature, the time required for isomerization reversal could be reduced from 3 to 2.5 h (Figure S4), suggesting a potential way for the utilization of waste heat.

3.3. Adsorption Performance. CO and N_2 adsorption properties of different samples were tested in a systematic manner. Adsorption experiments were initially carried out on the support Y (Figure S5). Due to the absence of a photo-responsive molecular SP, the amount of CO adsorbed did not change significantly (below 3%) both before and after visible light irradiation. Differently from carrier Y, the adsorption behavior of SP@Y on CO changed significantly after visible light irradiation, and all of them produced different degrees of decrease in CO uptake (Figures S6 and S7, Figure 4a,b). This is probably owing to the fact that CO molecules have smaller interactions with the SP isomerizes, which becomes less polar after visible light irradiation, and have stronger interactions with the more polar MC state, which is stabilized under dark storage. Take the representative sample 1SP@Y as an example, the amount of CO adsorbed in the MC isomerization at 25 °C and 1 bar is 7.0 $cm^3 \cdot g^{-1}$, whereas it decreased to 4.6 $cm^3 \cdot g^{-1}$ in the SP state upon visible light irradiation, a change equivalent to 34% of the adsorption capacity. Further increase in SP loading causes a decline in CO adsorption (i.e., 6.0 $cm^3 \cdot g^{-1}$ at 25 °C and 1 bar), which can be attributed to the higher loading of SP severely clogging the Y zeolite cavities, thereby limiting the total amount of CO that can be captured. At the same time, the responsiveness of the sample also decreased, which may be due to the dense packing of smaller pores, making it difficult for a portion of spiropyran molecules to undergo isomerization.[35,39] Additionally, by applying visible light during the test, the release of CO from 1SP@Y can be realized in situ, as shown in Figure S8. Besides, the adsorption of N_2 for 1SP@Y is essentially indistinguishable between the SP and MC states, which can be attributed to the fact that N_2, as a nonpolar molecule, responds to changes in the state of the molecule with little effect on its adsorption. To broaden the application of this strategy, NaY zeolite was used as a carrier, and 1SP@NaY was obtained through a process similar to that used for 1SP@Y. The adsorption properties of the obtained 1SP@NaY were then studied. The adsorption capacity of 1SP@NaY for CO was 6.1 $cm^3 \cdot g^{-1}$ in the MC state and 5 $cm^3 \cdot g^{-1}$ in the SP state (Figure S9), with a change of only 18%, which is less than that of 1SP@Y. This may be due to the absence of active sites in NaY that can interact with CO, whereas in Y, Ni^{2+} ions can act as active sites, selectively engaging with CO through π-complexation.[40,41] The incorporation of SP in its cavities facilitates a synergistic interaction with Ni^{2+}, thereby enhancing the adsorption capacity and regulatory effects on CO.

The ideal adsorption solution theory (IAST) model is specifically utilized to evaluate the gas selectivity (Figure 4c). On the optimal sample 1SP@Y, the selectivity of CO/N_2 in the MC state was 9.4, and upon visible light irradiation, the selectivity in the SP state decreased significantly to 3.2 (25 °C, 1 bar). In this way, it indicates that the selectivity of the smart adsorbent can be effectively adjusted via visible light irradiation. In order to ensure the cyclic regeneration ability of the adsorbent and the reproducibility of the photoresponse, 1SP@Y was tested cyclically. By alternating visible and dark light treatments, the SP was cyclically transformed between the two configurations to observe its adsorption behavior, as shown in Figure 4d. It can be seen that the light-induced changes in adsorption were reversible within 2.5 cycles. The above results show that the strategy that light can regulate the adsorption behavior of adsorbents is completely feasible.

DFT calculations were employed to reveal a potential mechanism for the tunable adsorption behavior. Figure S10 shows the optimized models for SP and MC. After that, an optimized model of CO molecules interacting in the presence of SP and MC molecules was carried out. The calculated binding energies to CO in the MC state and in the SP state are −22 and −20 kJ/mol, respectively, indicating that they can both interact with CO molecules through van der Waals forces. Since the binding energy of the MC state is less than that of the SP state, the MC state has a more intense electrostatic effect with CO and is more preferred to trap CO molecules. Therefore, the computational results are closely consistent with the experimental results. Calculations of binding energy are conducted within the context of an isolated system, yet dipole−dipole interactions exist between photo-responsive porous materials and polar molecules.[42] To investigate how photo-isomerization of responsive molecules influences the performance of porous hosts, dynamic contact angle measurements were performed on 1SP@Y (Figure S11). It was

https://doi.org/10.1021/cbe.4c00016
Chem Bio Eng. 2024, 1, 783−789

observed that the initial contact angle in the MC state was 65°, lower than that in the SP state (78°). Additionally, the contact angle in the MC state decreased significantly faster over time compared to the SP state, demonstrating stronger hydrophilicity. This suggests that the material in the MC state exhibits enhanced pore polarity, enabling stronger interactions with CO. Upon isomerization from MC to SP, the polarity within the pores of the host material decreases, leading to the release of CO. The observed differences in adsorption capacity may be attributed to the synergistic effects of binding energy and pore polarity.

4. CONCLUSIONS

In summary, we prepared visible-light-modulated CO smart adsorbents by in situ synthesizing SP in zeolite Y via the ship-in-the-bottle method. This avoids photo-responsive adsorbents that require UV modulation, which has the disadvantages of potential destructiveness and shallow penetration depth. The different binding strengths of MC and SP states in zeolite Y of the isomerization to CO lead to the variation of the adsorption of CO by SP@Y up to 34%. The reversible cycling test proved that the adsorbent had good reproducibility. DFT calculations demonstrated that the binding energies between the different isomeric states of the photo-responsive moieties and CO molecules were different, and MC tended to capture CO molecules more than SP. This strategy of combining light-responsive and traditional composite adsorbents provides a new perspective for the development of smart materials and the upgrading of traditional adsorbents.

■ ASSOCIATED CONTENT

Supporting Information

The Supporting Information is available free of charge at https://pubs.acs.org/doi/10.1021/cbe.4c00016.

Detailed experimental part, materials characterization, adsorption equilibrium model and selectivity, DFT calculations, SEM images, TG profiles, UV-Vis spectra of 1SP@Y, adsorption isotherms of CO and N_2 on 0.5SP@Y, 1.5SP@Y, and 1SP@NaY upon SP/MC isomerization, in situ dynamic liberation of CO on 1SP@Y, and dynamic water contact angles (PDF)

■ AUTHOR INFORMATION

Corresponding Author

Lin-Bing Sun − *State Key Laboratory of Materials-Oriented Chemical Engineering, Jiangsu National Synergetic Innovation Center for Advanced Materials (SICAM), College of Chemical Engineering, Nanjing Tech University, Nanjing 211816, P. R. China;* orcid.org/0000-0002-6395-312X; Email: lbsun@njtech.edu.cn

Authors

Shu Shi − *State Key Laboratory of Materials-Oriented Chemical Engineering, Jiangsu National Synergetic Innovation Center for Advanced Materials (SICAM), College of Chemical Engineering, Nanjing Tech University, Nanjing 211816, P. R. China*

Zi-Da Ma − *State Key Laboratory of Materials-Oriented Chemical Engineering, Jiangsu National Synergetic Innovation Center for Advanced Materials (SICAM), College of Chemical Engineering, Nanjing Tech University, Nanjing 211816, P. R. China*

Yu-Xia Li − *State Key Laboratory of Materials-Oriented Chemical Engineering, Jiangsu National Synergetic Innovation Center for Advanced Materials (SICAM), College of Chemical Engineering, Nanjing Tech University, Nanjing 211816, P. R. China;* orcid.org/0000-0003-1916-2707

Shi-Chao Qi − *State Key Laboratory of Materials-Oriented Chemical Engineering, Jiangsu National Synergetic Innovation Center for Advanced Materials (SICAM), College of Chemical Engineering, Nanjing Tech University, Nanjing 211816, P. R. China;* orcid.org/0000-0002-9609-7710

Complete contact information is available at: https://pubs.acs.org/10.1021/cbe.4c00016

Notes

The authors declare no competing financial interest.

■ ACKNOWLEDGMENTS

We acknowledge the financial support of this work by the National Natural Science Foundation of China (22078155 and 22178163) and the National Science Fund for Distinguished Young Scholars (22125804). We are grateful to the High-Performance Computing Center of Nanjing Tech University for supporting the computational resources.

■ REFERENCES

(1) Sholl, D. S.; Lively, R. P. Seven Chemical Separations to Change the World. *Nature* **2016**, *532*, 435−437.

(2) Li, J.-R.; Sculley, J.; Zhou, H.-C. Metal-Organic Frameworks for Separations. *Chem. Rev.* **2012**, *112*, 869−932.

(3) Motkuri, R. K.; Thallapally, P. K.; Annapureddy, H. V. R.; Dang, L. X.; Krishna, R.; Nune, S. K.; Fernandez, C. A.; Liu, J.; McGrail, B. P. Separation of Polar Compounds using a Flexible Metal-Organic Framework. *Chem. Commun.* **2015**, *51*, 8421−8424.

(4) Yang, L.; Qian, S.; Wang, X.; Cui, X.; Chen, B.; Xing, H. Energy-Efficient Separation Alternatives: Metal-Organic Frameworks and Membranes for Hydrocarbon Separation. *Chem. Soc. Rev.* **2020**, *49*, 5359−5406.

(5) Kitagawa, S. Porous Materials and the Age of Gas. *Angew. Chem. Int. Ed.* **2015**, *54*, 10686−10687.

(6) Reed, D. A.; Xiao, D. J.; Gonzalez, M. I.; Darago, L. E.; Herm, Z. R.; Grandjean, F.; Long, J. R. Reversible CO Scavenging via Adsorbate-Dependent Spin State Transitions in an Iron(II)-Triazolate Metal-Organic Framework. *J. Am. Chem. Soc.* **2016**, *138*, 5594−5602.

(7) Lin, J. Y. S. Molecular Sieves for Gas Separation. *Science* **2016**, *353*, 121−122.

(8) Jiang, Y.; Tan, P.; Liu, X. Q.; Sun, L. B. Process-Oriented Smart Adsorbents: Tailoring the Properties Dynamically as Demanded by Adsorption/Desorption. *Acc. Chem. Res.* **2022**, *55*, 75−86.

(9) Tan, P.; Jiang, Y.; Qi, S.-C.; Gao, X.-J.; Liu, X.-Q.; Sun, L.-B. Ce-Doped Smart Adsorbents with Photoresponsive Molecular Switches for Selective Adsorption and Efficient Desorption. *Engineering* **2020**, *6*, 569−576.

(10) Choi, W.; Min, K.; Kim, C.; Ko, Y. S.; Jeon, J. W.; Seo, H.; Park, Y.-K.; Choi, M. Epoxide-Functionalization of Polyethyleneimine for Synthesis of Stable Carbon Dioxide Adsorbent in Temperature Swing Adsorption. *Nat. Commun.* **2016**, *7*, 12640.

(11) Wu, Q. R.; Tan, P.; Gu, C.; Zhou, R.; Qi, S. C.; Liu, X. Q.; Jiang, Y.; Sun, L. B. Smart Adsorbents for CO_2 Capture: Making Strong Adsorption Sites Respond to Visible Light. *Sci. China Mater.* **2021**, *64*, 383−392.

(12) Tan, P.; Jiang, Y.; Liu, X. Q.; Sun, L. B. Making Porous Materials Respond to Visible Light. *ACS Energy Lett.* **2019**, *4*, 2656−2667.

(13) Zhao, Y.; Bai, G.; Huang, Y.; Liu, Y.; Peng, D.; Chen, L.; Xu, S. Stimuli Responsive Lanthanide Ions Doped Layered Piezophotonic

Microcrystals for Optical Multifunctional Sensing Applications. *Nano Energy* **2021**, *87*, 106177.
(14) Cai, W.; Wang, J.; Chu, C.; Chen, W.; Wu, C.; Liu, G. Metal-Organic Framework-Based Stimuli-Responsive Systems for Drug Delivery. *Adv. Sci.* **2019**, *6*, 1801526.
(15) Zhang, J.; Zhang, M.; Tang, K.; Verpoort, F.; Sun, T. Polymer-Based Stimuli-Responsive Recyclable Catalytic Systems for Organic Synthesis. *Small* **2014**, *10*, 32−46.
(16) Li, M.; Liu, J.; Tan, P.; Liu, X. Q.; Sun, L. B. Photomodulation on Adsorptive Desulfurization by Ag(0): Photothermal Active Sites with High Stability. *AIChE J.* **2023**, *69*, No. e18034.
(17) Guan, Q.; Fang, Y.; Wu, X.; Ou, R.; Zhang, X.; Xie, H.; Tang, M.; Zeng, G. Stimuli Responsive Metal Organic Framework Materials towards Advanced Smart Application. *Mater. Today* **2023**, *64*, 138−164.
(18) Meng, X.; Qi, G.; Li, X.; Wang, Z.; Wang, K.; Zou, B.; Ma, Y. Spiropyran-Based Multi-Colored Switching Tuned by Pressure and Mechanical Grinding. *J. Mater. Chem. C* **2016**, *4*, 7584−7588.
(19) Ou, R.; Zhang, H.; Truong, V. X.; Zhang, L.; Hegab, H. M.; Han, L.; Hou, J.; Zhang, X.; Deletic, A.; Jiang, L.; Simon, G. P.; Wang, H. A Sunlight-Responsive Metal-Organic Framework System for Sustainable Water Desalination. *Nat. Sustain.* **2020**, *3*, 1052−1058.
(20) Kundu, P. K.; Samanta, D.; Leizrowice, R.; Margulis, B.; Zhao, H.; Borner, M.; Udayabhaskararao, T.; Manna, D.; Klajn, R. Light-Controlled Self-Assembly of Non-Photoresponsive Nanoparticles. *Nat. Chem.* **2015**, *7*, 646−652.
(21) Gu, Y.; Alt, E. A.; Wang, H.; Li, X.; Willard, A. P.; Johnson, J. A. Photoswitching Topology in Polymer Networks with Metal-Organic Cages as Crosslinks. *Nature* **2018**, *560*, 65−69.
(22) Garg, S.; Schwartz, H.; Kozlowska, M.; Kanj, A. B.; Muller, K.; Wenzel, W.; Ruschewitz, U.; Heinke, L. Conductance Photoswitching of Metal-Organic Frameworks with Embedded Spiropyran. *Angew. Chem. Int. Ed.* **2019**, *58*, 1193−1197.
(23) Crespi, S.; Simeth, N. A.; Konig, B. Heteroaryl Azo Dyes as Molecular Photoswitches. *Nat. Rev. Chem.* **2019**, *3*, 133−146.
(24) Rice, A. M.; Martin, C. R.; Galitskiy, V. A.; Berseneva, A. A.; Leith, G. A.; Shustova, N. B. Photophysics Modulation in Photoswitchable Metal-Organic Frameworks. *Chem. Rev.* **2020**, *120*, 8790−8813.
(25) Thaggard, G. C.; Haimerl, J.; Park, K. C.; Lim, J.; Fischer, R. A.; Maldeni Kankanamalage, B. K. P.; Yarbrough, B. J.; Wilson, G. R.; Shustova, N. B. Metal-Photoswitch Friendship: From Photochromic Complexes to Functional Materials. *J. Am. Chem. Soc.* **2022**, *144*, 23249−23263.
(26) Gemen, J.; Church, J. R.; Ruoko, T.-P.; Durandin, N.; Białek, M.ł J.; Weißenfels, M.; Feller, M.; Kazes, M.; Odaybat, M.; Borin, V. A.; Kalepu, R.; Diskin-Posner, Y.; Oron, D.; Fuchter, M. J.; Priimagi, A.; Schapiro, I.; Klajn, R. Disequilibrating Azobenzenes by Visible-Light Sensitization under Confinement. *Science* **2023**, *381*, 1357−1363.
(27) Bléger, D.; Schwarz, J.; Brouwer, A. M.; Hecht, S. o-Fluoroazobenzenes as Readily Synthesized Photoswitches Offering Nearly Quantitative Two-Way Isomerization with Visible Light. *J. Am. Chem. Soc.* **2012**, *134*, 20597−20600.
(28) Beharry, A. A.; Sadovski, O.; Woolley, G. A. Azobenzene Photoswitching without Ultraviolet Light. *J. Am. Chem. Soc.* **2011**, *133*, 19684−19687.
(29) Liang, H. Q.; Guo, Y.; Shi, Y.; Peng, X.; Liang, B.; Chen, B. A Light-Responsive Metal-Organic Framework Hybrid Membrane with High On/Off Photoswitchable Proton Conductivity. *Angew. Chem. Int. Ed.* **2020**, *59*, 7732−7737.
(30) Klajn, R. Spiropyran-Based Dynamic Materials. *Chem. Soc. Rev.* **2014**, *43*, 148−184.
(31) Chen, S.; Jiang, F.; Cao, Z.; Wang, G.; Dang, Z.-M. Photo, pH, and Thermo Triple-Responsive Spiropyran-Based Copolymer Nanoparticles for Controlled Release. *Chem. Commun.* **2015**, *51*, 12633−12636.
(32) Bletz, M.; Pfeifer-Fukumura, U.; Kolb, U.; Baumann, W. Ground- and First-Excited-Singlet-State Electric Dipole Moments of Some Photochromic Spirobenzopyrans in Their Spiropyran and Merocyanine Form. *J. Phys. Chem. A* **2002**, *106*, 2232−2236.
(33) Shiraishi, Y.; Shirakawa, E.; Tanaka, K.; Sakamoto, H.; Ichikawa, S.; Hirai, T. Spiropyran-Modified Gold Nanoparticles: Reversible Size Control of Aggregates by UV and Visible Light Irradiations. *ACS Appl. Mater. Interfaces* **2014**, *6*, 7554−7562.
(34) Healey, K.; Liang, W.; Southon, P. D.; Church, T. L.; D'Alessandro, D. M. Photoresponsive Spiropyran-Functionalised MOF-808: Postsynthetic Incorporation and Light Dependent Gas Adsorption Properties. *J. Mater. Chem. A* **2016**, *4*, 10816−10819.
(35) Shi, S.; Li, K.-D.; Li, Y. X.; Ma, Z. D.; Qi, S. C.; Liu, X. Q.; Sun, L. B. Spiropyran-Embedded Metal-Organic Frameworks with Thermoresponsiveness for Tunable Gas Adsorption. *ACS Mater. Lett.* **2023**, *5*, 2189−2196.
(36) Casades, I.; Constantine, S.; Cardin, D.; Garcıa, H.; Gilbert, A.; Marquez, F. 'Ship-in-a-Bottle' Synthesis and Photochromism of Spiropyrans Encapsulated within Zeolite Y Supercages. *Tetrahedron* **2000**, *56*, 6951−6956.
(37) Kahle, I.; Spange, S. Internal and External Acidity of Faujasites As Measured by a Solvatochromic Spiropyran. *J. Phys. Chem. C* **2010**, *114*, 15448−15453.
(38) Schwartz, H. A.; Schaniel, D.; Ruschewitz, U. Tracking the Light-Induced Isomerization Processes and the Photostability of Spiropyrans Embedded in the Pores of Crystalline Nanoporous MOFs via IR Spectroscopy. *Photochem. Photobiol. Sci.* **2020**, *19*, 1433−1441.
(39) Kundu, P. K.; Olsen, G. L.; Kiss, V.; Klajn, R. Nanoporous Frameworks Exhibiting Multiple Stimuli Responsiveness. *Nat. Commun.* **2014**, *5*, 3588.
(40) Khan, N. A.; Jhung, S. H. Adsorptive Removal and Separation of Chemicals with Metal-Organic Frameworks: Contribution of π-Complexation. *J. Hazard. Mater.* **2017**, *325*, 198−213.
(41) Oliveira, M. L. M.; Miranda, A. A. L.; Barbosa, C. M. B. M.; Cavalcante, C. L.; Azevedo, D. C. S.; Rodriguez-Castellon, E. Adsorption of Thiophene and Toluene on NaY Zeolites Exchanged with Ag(I), Ni(II) and Zn(II). *Fuel* **2009**, *88*, 1885−1892.
(42) Wang, Z.; Grosjean, S.; Brase, S.; Heinke, L. Photoswitchable Adsorption in Metal-Organic Frameworks Based on Polar Guest-Host Interactions. *ChemPhysChem* **2015**, *16*, 3779−3783.

https://doi.org/10.1021/cbe.4c00016
Chem Bio Eng. 2024, 1, 783−789